Grapevine MATE-type proteins act as vacuolar H+-dependent acylated anthocyanin transporters

Camila Gomez, Nancy N. Terrier, Laurent Torregrosa, Sandrine S. Vialet, Alexandre Fournier Level, Clotilde Verries, Jean Marc J. M. Souquet, Jean Paul Mazauric, Markus Klein, Veronique V. Cheynier, et al.

Grapevine MATE-Type Proteins Act as Vacuolar H^+-Dependent Acylated Anthocyanin Transporters[1][W][OA]

Camila Gomez, Nancy Terrier, Laurent Torregrosa, Sandrine Vialet, Alexandre Fournier-Level, Clotilde Verriès, Jean-Marc Souquet, Jean-Paul Mazauric, Markus Klein[2], Véronique Cheynier, and Agnès Ageorges*

UMR Sciences pour l'Œnologie, INRA Campus SupAgro, F–34060 Montpellier, France (C.G., N.T., S.V., C.V., J.-M.S., J.-P.M., V.C., A.A.); UMR Diversité et Adaptation des Plantes Cultivées 1097, INRA Campus SupAgro, F–34060 Montpellier, France (L.T., A.F.-L.); and Zurich Basel Plant Science Center, University of Zurich, Plant Biology, CH–8008 Zurich, Switzerland (M.K.)

In grapevine (*Vitis vinifera*), anthocyanins are responsible for most of the red, blue, and purple pigmentation found in the skin of berries. In cells, anthocyanins are synthesized in the cytoplasm and accumulated into the vacuole. However, little is known about the transport of these compounds through the tonoplast. Recently, the sequencing of the grapevine genome allowed us to identify genes encoding proteins with high sequence similarity to the Multidrug And Toxic Extrusion (MATE) family. Among them, we selected two genes as anthocyanin transporter candidates and named them *anthoMATE1* (*AM1*) and *AM3*. The expression of both genes was mainly fruit specific and concomitant with the accumulation of anthocyanin pigment. Subcellular localization assays in grapevine hairy roots stably transformed with AM1:: or AM3::green fluorescent protein fusion protein revealed that AM1 and AM3 are primarily localized to the tonoplast. Yeast vesicles expressing anthoMATEs transported acylated anthocyanins in the presence of MgATP. Inhibitor studies demonstrated that AM1 and AM3 proteins act in vitro as vacuolar H^+-dependent acylated anthocyanin transporters. By contrast, under our experimental conditions, anthoMATEs could not transport malvidin 3-*O*-glucoside or cyanidin 3-*O*-glucoside, suggesting that the acyl conjugation was essential for the uptake. Taken together, these results provide evidence that in vitro the two grapevine AM1 and AM3 proteins mediate specifically acylated anthocyanin transport.

Anthocyanins are plant secondary metabolites, responsible for most of the red, blue, and purple pigmentation found in flowers, fruits, and leaves (Harborne and Williams, 2000). They are involved in plant resistance against UV light and in animal attraction for pollination and seed dissemination. In vivo, anthocyanins are accumulated in the vacuole, which offers a large storage space allowing anthocyanins to reach concentrations high enough to confer physiological and ecological advantages to plants while avoiding harmful effects (Archetti, 2000; Manetas, 2006). From a structural standpoint, anthocyanins are glycosylated derivatives of aglycone chromophores, called anthocyanidins, that differ from each other by the number of hydroxyl and methoxyl groups. Further diversity arises from the nature of the sugar(s) and from its acylation. These substitutions, catalyzed by glycosyltransferases, methyltransferases, and acyltransferases, increase the chemical stability of anthocyanins and confer to them many of their chemical and bioactive properties (Winefield, 2002). Acylated anthocyanins and especially those acylated with aromatic acids are exceptionally resistant to discoloration (Dangles et al., 1993; Cheynier et al., 2006). Grapevine (*Vitis vinifera*) anthocyanins are the 3-monoglucosides of five anthocyanidins: cyanidin, delphinidin and its methylated derivatives, peonidin, petunidin, and malvidin. In addition, the glucosyl group is found acylated with acetyl, *p*-coumaroyl, and, to a lesser extent, caffeoyl residues. Overall, the predominant anthocyanin in red grape cultivars is malvidin 3-*O*-glucoside (M3G). Nevertheless, the anthocyanin profiles show large varietal diversity and have been used as chemotaxonomy criteria (Roggero et al., 1988). In particular, the proportions of acylated anthocyanins are varietal characteristics. In grapevine berry, anthocyanins are accumulated in the skin of red cultivars. During berry development, the accumulation begins at véraison, and the anthocyanin content increases until ripening (Boss et al., 1996).

In plants, anthocyanins are part of the flavonoid biosynthetic pathway, which is one of the most intensively studied in plants (Winkel-Shirley, 2001). As a

[1] This work was supported by the European Union program FLAVO 2005–513960.

[2] Present address: Philip Morris International, R&D, Quai Jeanrenaud 56, 2000 Neuchâtel, Switzerland.

* Corresponding author; e-mail ageorges@supagro.inra.fr.

The author responsible for distribution of materials integral to the findings presented in this article in accordance with the policy described in the Instructions for Authors (www.plantphysiol.org) is: Agnès Ageorges (ageorges@supagro.inra.fr).

[W] The online version of this article contains Web-only data.

[OA] Open Access articles can be viewed online without a subscription.

www.plantphysiol.org/cgi/doi/10.1104/pp.109.135624

result, most of the structural genes as well as a number of regulatory genes have now been characterized (Winkel-Shirley, 2001; Broun, 2005), but little is known about the molecular mechanisms involved in the downstream steps of the pathway, including flavonoid accumulation into the vacuole. In the cell, anthocyanins are believed to be synthesized at the cytosolic surface of the endoplasmic reticulum (ER) by a multienzyme complex, although the association of anthocyanin enzymes with the ER membrane has not been fully established (Saslowsky and Winkel-Shirley, 2001). With regard to transport from the cytoplasmic surface of the ER to the vacuole, Grotewold and Davies (2008) suggested two models, a vesicular transport (VT) model and a ligandin transporter (LT) model. The VT model may be a direct trafficking route from the ER to the vacuole involving vesicle-like structures filled with anthocyanins. Recently, in Arabidopsis (*Arabidopsis thaliana*) seedlings, anthocyanins were shown to be sequestered in cytoplasmic structures that resemble ER-derived vesicle-like structures (Poustka et al., 2007). In *Lisianthus* petals and maize (*Zea mays*) cell suspension, anthocyanins were accumulated as vesicle-like bodies in the cytoplasm, suggesting a transport under this form to the vacuole (Grotewold et al., 1998; Zhang et al., 2006), although the presence of membranes around such structures remains to be determined. The LT model appears to involve ligandins that bind and escort anthocyanins from the biosynthesis site to the tonoplast, where they are supposed to enter the vacuole through tonoplast transporters.

Two major mechanisms have been proposed for transport across the tonoplast, primary transport mediated by ATP-binding cassette (ABC) transporters (Lu et al., 1998; Goodman et al., 2004; Verrier et al., 2008) and secondary transport depending on the H^+ gradient (Martinoia et al., 2007). Several lines of evidence indicated the involvement of primary multidrug resistance-associated protein (MRP)-type ABC transporters in the vacuolar accumulation of phenolic compounds (Klein et al., 2006). Most importantly, a maize antisense mutant of a vacuole-localized ABCC subfamily member (Verrier et al., 2008), ZmMRP3, exhibited a reduction in anthocyanin production and pigment mislocalization (Goodman et al., 2004). The main secondary transport mechanism depends on a preexisting H^+ gradient across the vacuolar membrane generated by V-ATPase and vacuolar H^+-pyrophosphatase (Klein et al., 1996). Recently, Verweij et al. (2008) described a P-ATPase proton pump on the tonoplast involved in vacuolar acidification in petunia (*Petunia hybrida*) petals that likely provides the proton gradient across the membrane used to energize anthocyanin uptake. In flavonoid transport, the uptake of acylated anthocyanins into isolated vacuoles of carrot (*Daucus carota*) cell suspension culture was inhibited by protonophores, suggesting dependence on a proton gradient (Hopp and Seitz, 1987), which is in accordance with results in barley (*Hordeum vulgare*), where vacuolar flavonoid glucoside uptake was also described as a ΔpH-dependent mechanism (Klein et al., 1996). In line with this second transporter family, Multidrug And Toxic Extrusion (MATE) transporters have been identified as candidate carrier proteins for flavonoid/H^+ exchange (Yazaki, 2005). The Arabidopsis gene *TT12* encodes a MATE protein required for proanthocyanidin sequestration into the vacuole of the seed coat endothelium (Debeaujon et al., 2001). Marinova et al. (2007) demonstrated that TT12 is necessary for vacuolar accumulation of proanthocyanidins and has been shown to mediate anthocyanin transport in vitro. Interestingly, the MATE transporter gene *MTP77* related to *TT12* was overexpressed in tomato (*Solanum lycopersicum*) fruit, up-regulating a MYB-type transcription factor (*ANT1*) triggering anthocyanin hyperaccumulation (Mathews et al., 2003).

In grapevine, no experimental evidence supporting the existence of the VT and/or the LT model is available. A glutathione *S*-transferase (GST) whose gene expression pattern is coordinated with color development was identified in grape berries (Ageorges et al., 2006). Recently, Conn et al. (2008) showed that this GST complements the maize mutant *bz2* characterized by a bronze color, resulting from a mislocalization of anthocyanins in the cytosol (Marrs et al., 1995). This result confirms the involvement of GST in vacuolar sequestration of anthocyanins. Circumstantial evidence suggests that two distinct transporters are involved in grape vacuolar anthocyanin transport: (1) a translocator homologous to the mammalian bilitranslocase was identified in grape berries using an anti-bilitranslocase antibody (Braidot et al., 2008); (2) high-throughput expression analysis revealed that the ectopic expression of transcription factor *VlmybA1-2* in grapevine hairy roots induced the expression of a candidate gene encoding a protein highly similar to MATE proteins (Cutanda-Perez et al., 2009). In this work, we describe the identification and biochemical characterization of two grapevine MATE transporters. The expression of these two genes was concomitant with anthocyanin accumulation in grape berry. These genes encoded proteins that are targeted to the tonoplast and were able to selectively transport acylated anthocyanins. The biochemical characterization of the transport activity suggests that these two MATE transporters are responsible for the vacuolar transport of acylated anthocyanins in grapevine.

RESULTS

Structure of *AnthoMATE* Genes and in Silico Analysis of Deduced Proteins

From the grapevine genome sequence (Jaillon et al., 2007) we identified 65 genes encoding proteins with high sequence similarity to MATE family proteins (Fig. 1). The phylogenetic tree was created after the alignment of full-length amino acid sequences of all identified grapevine MATEs and of the previously described plant MATEs: MTP77, the putative antho-

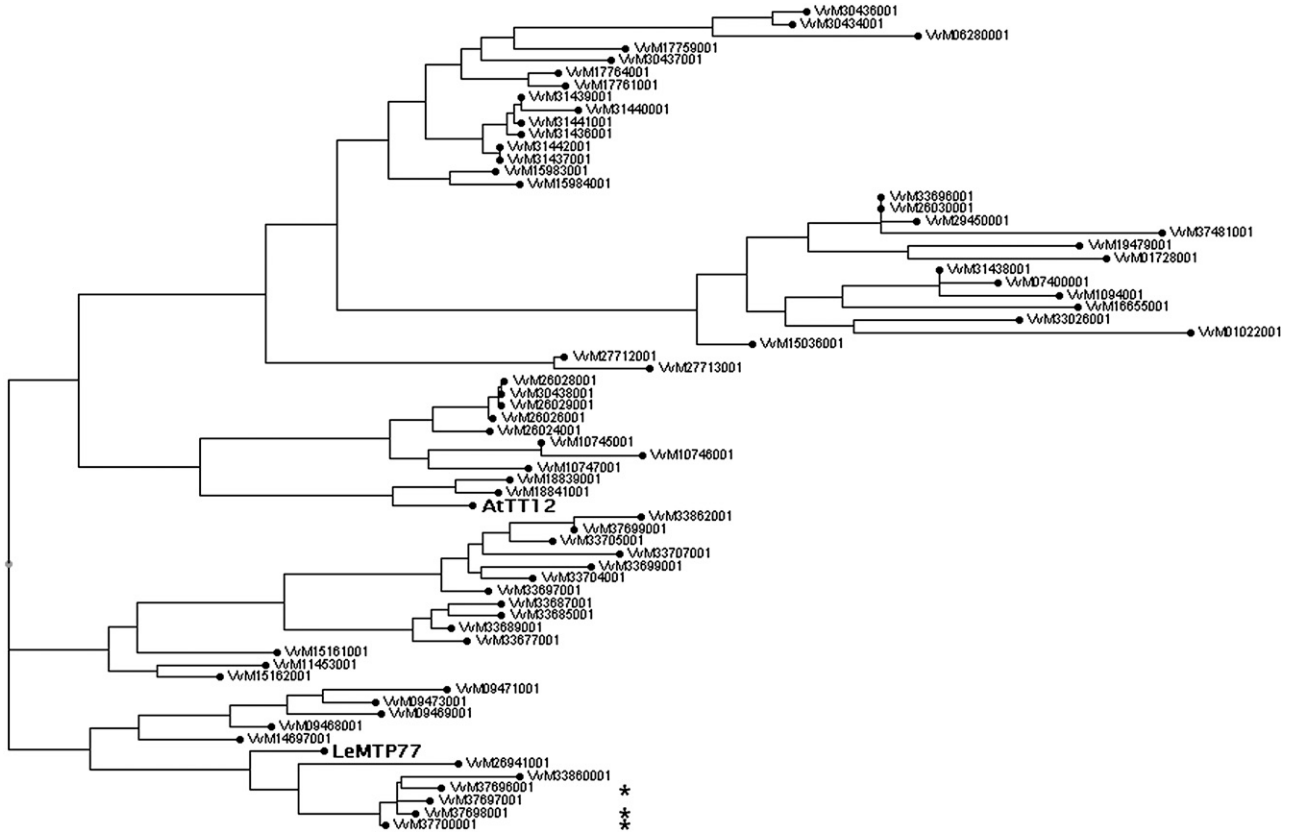

Figure 1. Phylogenetic tree of the predicted amino acid sequences of grapevine MATE proteins, Arabidopsis TT12 (Q9LYT3), and tomato MTP77 (AAQ55183). The asterisks indicate genes selected as being putative anthocyanin transporters. In the accession numbers of grapevine sequences annotated in the Genoscope grape genome browser (http://www.genoscope.cns.fr/vitis/; data obtained from the 8-fold coverage of the genome), "GSVIVP000" was simplified to "VvM." Relative similarities between sequences (proportional to horizontal branch lengths) are drawn to scale.

cyanin transporter in tomato (Mathews et al., 2003), and TT12, the Arabidopsis proanthocyanidin precursor transporter (Debeaujon et al., 2001). The phylogenetic tree clearly indicated three distinct clusters, where TT12 and MTP77 are grouped in different clusters (Fig. 1). The cluster including TT12 contained 10 grapevine MATE proteins, where two were closely related to TT12 (GSVIVP00018841001 and GSVIVP00018839001). The MTP77 cluster included 27 proteins and was split into two branches. Six putative MATEs were closely related to MTP77 (GSVIVP00037700001, GSVIVP00037698001, GSVIVP00037696001, GSVIVP0003386001, GSVIVP00026941001, and GSVIVP00037697001; Fig. 1). The three proteins presenting the highest similarity with MTP77, a putative anthocyanin transporter of tomato, were selected as candidates involved in anthocyanin transport in grape berry and named as anthoMATEs: AM1 (GSVIVP00037700001), AM2 (GSVIVP00037698001), and AM3 (GSVIVP00037696001). Alignment of the sequences of these three proteins showed that AM1, AM2, and AM3 exhibited 70%, 73%, and 72% nucleotide sequence identity with MTP77, respectively, and 69%, 70%, and 67% amino acid sequence similarity with MTP77, respectively. All three are located in the same scaffold of the Genoscope genome browser database (Fig. 2). The gene structures as predicted by the Genoscope genome browser suggested that the genomic DNAs of GSVIVT00037700001 (*AM1*), GSVIVT00037698001 (*AM2*), and GSVIVT00037696001 (*AM3*) are 3,079, 2,997, and 2,901 bp long, respectively.

From Syrah mature berries, full-length cDNAs for *AM1* and *AM3* were amplified by reverse transcription-PCR, cloned, and fully sequenced. In contrast, all our attempts to clone *AM2* were not successful, suggesting that *AM2* was probably not expressed at detectable levels in mature berry or was a pseudogene. *AM1* and *AM3* transcripts were 1,482 and 1,470 nucleotides long, respectively, coding for polypeptides of 493 and 489 amino acid residues with predicted molecular masses of 53.85 and 53.50 kD and calculated pI values of 6.53 and 5.89, respectively (Fig. 3). The proteins exhibited 86% identity to each other. The prediction of transmembrane domains using the transmembrane hidden Markov model suggested 12 putative transmembrane segments for AM1 and AM3. This structure was similar to those of TT12 and MTP77 (Fig. 3). The Pfam database predicted for both AM1 and AM3 an

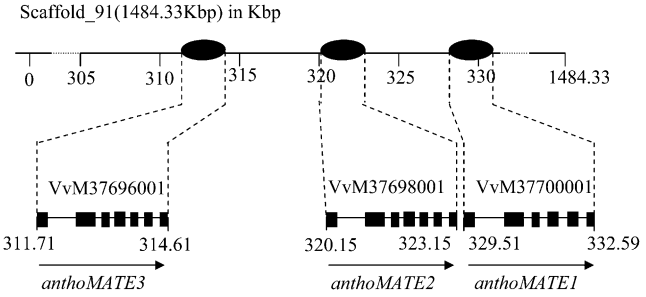

Figure 2. Genomic structures of *anthoMATE* genes in scaffold_91 of the Genoscope genome browser database (http://www.genoscope.cns.fr). The black boxes indicate exons. In the accession numbers annotated in the Genoscope grape genome browser (http://www.genoscope.cns.fr/vitis/; data obtained from the 8-fold coverage of the genome), "GSVIVT000" was simplified to "VvM."

architecture with two MatE domains (PF01554). The predicted MatE domain is highly similar to the MatE domain of MTP77, while less similarity was found for TT12. Five domains (D1–D5) appeared to be particularly conserved. Interestingly, D3 was located in transmembrane segment 7, while all other conserved domains were positioned in cytoplasmic loops.

AnthoMATE Protein Localization

To examine the subcellular localization of anthoMATE proteins, the full-length *AM1* and *AM3* cDNAs were fused at their C termini to GFP under the control of the cauliflower mosaic virus 35S promoter. The in vivo localization of both anthoMATE proteins was performed in hairy root cultures of grapevine stably transformed with GFP fusions and, as a control, with GFP alone. Confocal microscopy analysis of hairy roots ectopically expressing the transgenes *AM1*::*GFP* and *AM3*::*GFP* was performed after plasmolysis of cells with sorbitol and counterstaining of nuclei with 4′,6-diamino-phenylindole (DAPI; Fig. 4). Epidermal cells of hairy roots expressing *anthoMATE-GFP* fusions exhibited intracellular membrane-bound GFP fluorescence that internally surrounded the nucleus (Fig. 4, B and C). Gentle plasmolysis separates tonoplast from the cell wall and demonstrates clearly that the GFP fluorescence surrounds the vacuole and thus localizes to the tonoplast (Fig. 4, D and E). GFP fluorescence in membrane structures attached to the nucleus was also detected for AM1::GFP and AM3::GFP compared with GFP alone, where fluorescence was observed only in the cytosol (Fig. 4). Transient expression by biolistic particle delivery of *AM1*::*GFP* fusion together with the established tonoplast marker *TPK1* (Czempinski et al., 2002) fused to *DsRed2* in onion (*Allium cepa*) bulb epidermal cells confirmed that proteins coreside on vacuolar membranes (Supplemental Fig. S1A). We conclude that AM1 and AM3 are primarily localized to the tonoplast under our experimental conditions, even if we cannot exclude their presence on other endomembranes.

AnthoMATE Gene Expression

In order to define changes in expression associated with anthocyanin biosynthesis in grapevine berry, quantitative real-time PCR was performed on both *anthoMATE* genes during Syrah berry development. Both *anthoMATE* genes followed similar expression patterns during berry development (Fig. 5, A and B). Before the onset of ripening, *AM1* and *AM3* were hardly detectable in berry. After véraison, an increase of expression during the ripening stage was observed for both *anthoMATE* genes (Fig. 5, A and B). The expression profiles for *AM1* and *AM3* genes throughout berry development were correlated to the biosynthesis of anthocyanins. *AnthoMATE* gene expression was then evaluated in several tissues (Fig. 5, C and D). While *AM1* transcript was found at low levels in young and old leaves, no *AM3* expression was measured in leaves. In the other vegetative organs, both *AM1* and *AM3* transcripts were weakly present. Moreover, *AM1* and *AM3* expression was quite restricted to berry skin, where anthocyanin biosynthesis takes place (Fig. 5, C and D).

In order to investigate changes in expression in relation to anthocyanin composition in mature berries, the expression of both genes was also monitored on a set of 15 cultivars (Fig. 6). The berry samples were selected among white, pink, and red cultivars in order to maximize the phenotypic variation for anthocyanin content (Fig. 6A). Biochemical analysis showed a significant diversity in anthocyanin metabolites within the studied cultivars (Supplemental Table S1). In all cultivars, *AM1* expression was observed, and the expression level was independent of the anthocyanin content and composition in the berry samples (Fig. 6C). Conversely, *AM3* exhibited a higher expression in the red cultivars than in the other cultivars (Fig. 6D). When the ratio of acylated anthocyanin to total anthocyanin content in mature berry skins was compared with the expression patterns, it became evident that *AM3* expression correlates with the presence of acylated anthocyanins rather than the total anthocyanin content (Fig. 6, B and D). Indeed, expression of *AM3* was very weak in all white and pink cultivars, except for Roussaitis. This cultivar was the only pink cultivar containing all of the glucosylated anthocyanins plus petunidin 3-acetylglucoside and malvidin 3-*p*-coumaroylglucoside; all others contained only cyanidin 3-*O*-glucoside (C3G; Supplemental Table S1). A correlation of the level of expression of *AM3* with the ratio of acylated anthocyanin to total anthocyanin content was found (Pearson test $r = 0.75$, significant at $P = 0.0015$).

Overall, the expression of *AM1* and *AM3* was essentially fruit specific and concomitant with the accumulation of anthocyanin pigments. Moreover, *AM3* expression in mature berry was correlated with the percentage of acylated anthocyanin contained in berry.

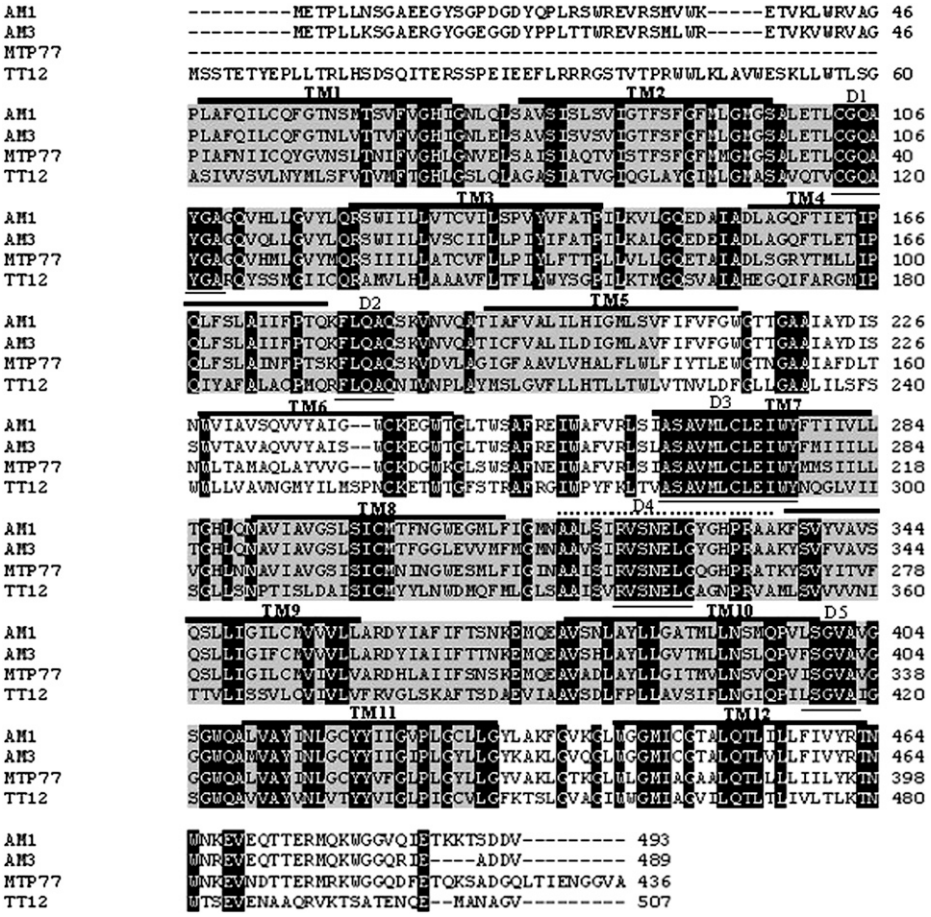

Figure 3. Alignment of AM1 and AM3 proteins with Arabidopsis TT12 and tomato MTP77 using the ClustalW program with default parameters. The MatE domain (PF01554) using the Pfam database is shown with gray background. The putative transmembrane segments (TM1–TM12) of anthoMATE proteins, using the HMMTOP program, are delimited by thick lines above the sequences. Conserved residues in all sequences are shown with black background. Conserved protein domains (D1–D5) are represented by thin lines below the sequences. The anthoMATE motif used in antibody synthesis is indicated by the dotted line.

AnthoMATE Protein in Vitro Transport Experiments

To investigate the transport activity of anthoMATE proteins, the full-length *AM1* and *AM3* cDNAs were expressed in *Saccharomyces cerevisiae* under the control of the constitutive *PMA1* promoter on a 2μ plasmid. Control experiments were performed in parallel with yeast transformed with the empty vector and with *TT12* (Marinova et al., 2007). Total microsomal membrane vesicles were isolated from the transgenic yeast, since Marinova et al. (2007) demonstrated that the transgene is not only restricted to the vacuolar membrane but is also present on other endomembranes and the plasma membrane. Western blot analysis performed on the isolated membrane vesicles with anti-anthoMATE antibodies confirmed the presence of anthoMATE proteins in the yeast transformants tested (Supplemental Fig. S2A). Furthermore, the physiological tightness of independent vesicle preparations was checked through the measurement of MgATP-dependent proton pumping by quenching of 9-amino-6-chloro-2-methoxyacridine (ACMA) fluorescence (Supplemental Fig. S2, B–E).

Transport experiments with various substrates were performed with a standard substrate concentration of 1 mM using the rapid filtration technique (Tommasini et al., 1996). The selected substrates were C3G, M3G, and an acylated anthocyanin mixture extracted and purified from Syrah grape berries. The acylated anthocyanin mixture contained mainly 3-*p*-coumaroylglucosylated anthocyanins and small amounts of malvidin 3-acetylglucosyl. With the different substrates, the empty vector-derived vesicles showed only a slight accumulation both in the presence and in the absence of MgATP, possibly due to an unspecific binding of substrate to membranes.

In the presence of MgATP and using either C3G or M3G, the amount of vesicle-associated substrates remained unchanged for anthoMATEs- or empty vector-derived vesicles (Fig. 7, A and B). These results suggest that, under our experimental conditions, C3G and

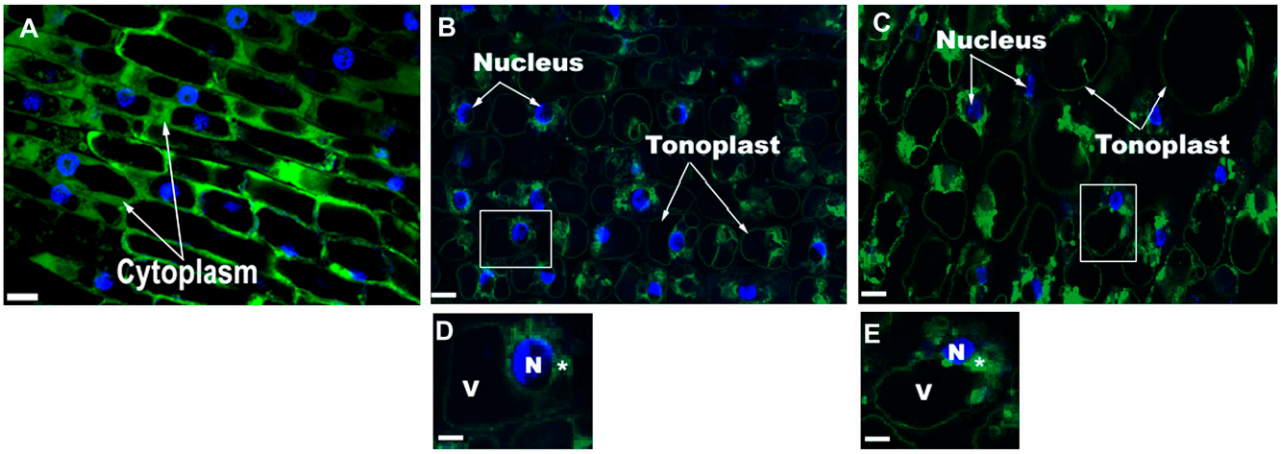

Figure 4. Subcellular localization of anthoMATE proteins after stable expression in grapevine hairy roots. Confocal microscopy images show grapevine root epidermal cells expressing nontargeted GFP protein (A), AM1::GFP fusion (B and D), and AM3::GFP fusion (C and E). Cells were plasmolyzed with 0.3 M sorbitol, and DNA was stained blue with DAPI and green with GFP. A, GFP fluorescence is visible in the cytoplasm. B to E, GFP fluorescence is visible on the tonoplast and in membrane structures attached to the nucleus (indicated by asterisks). N, Nucleus; V, vacuole. D and E show magnified images corresponding to the boxed regions in B and C, respectively. The image in C overlaid by differential interference contrast transmitted light is shown in Supplemental Figure S1B. Bars = 5 μm in A to C and 2 μm in D and E.

M3G were not transported by either anthoMATE protein (Fig. 7, A and B).

In a second experiment, we used the acylated anthocyanin mixture as a substrate for anthoMATE-dependent transport. In the presence of MgATP, vesicles expressing AM1 or AM3 exhibited an increase in their A_{536} (λ_{max} for malvidin 3-*p*-coumaroylglucoside) after 1 min of transport, suggesting an uptake of this compound (Fig. 7, A and B). In the presence of MgATP, a time-dependent increase in absorption occurred when the acylated anthocyanin mixture was incubated with AM1- and AM3-containing vesicles when compared with empty vector-derived vesicles, whose absorption remained unchanged over time (Fig. 7, C and D). HPLC analysis of the anthocyanins recovered from vesicles containing anthoMATE proteins after incubation with the acylated anthocyanins showed that transport occurs in the presence of MgATP as an energy source only (Fig. 7E). Taken together, these results indicate that acylated anthocyanins were selectively transported into vesicles by both anthoMATE proteins and when energization by MgATP occurred (Fig. 8).

To validate our experimental conditions, we performed the same test using TT12-containing vesicles

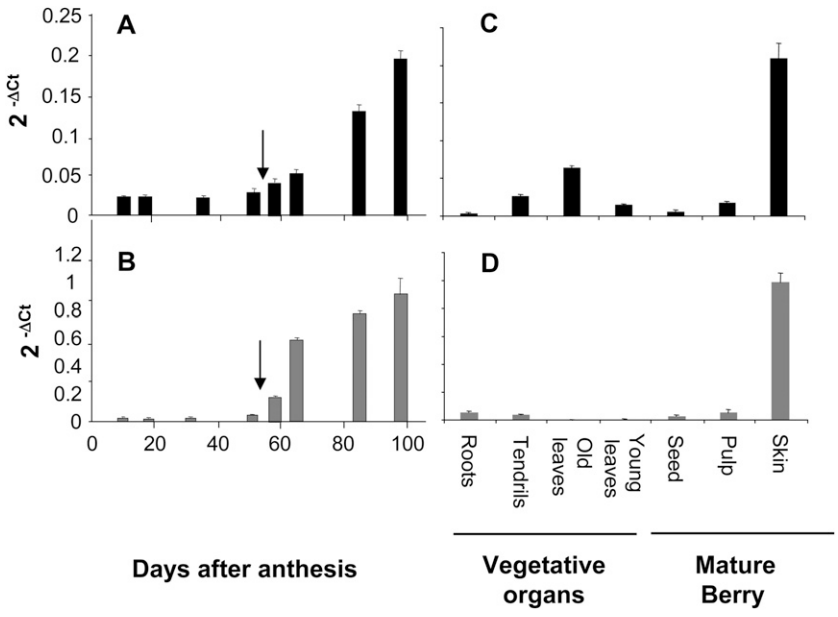

Figure 5. Quantitative real-time PCR expression profiling of *AM1* and *AM3*. Transcript levels of *AM1* (A) and *AM3* (B) during berry development (Syrah) and transcript levels of *AM1* (C) and *AM3* (D) in various grapevine organs and different tissues of mature berries are shown. The arrows indicate the véraison. Gene expression was normalized with *VvEF1α*. All data are means of three replicates with error bars indicating SD.

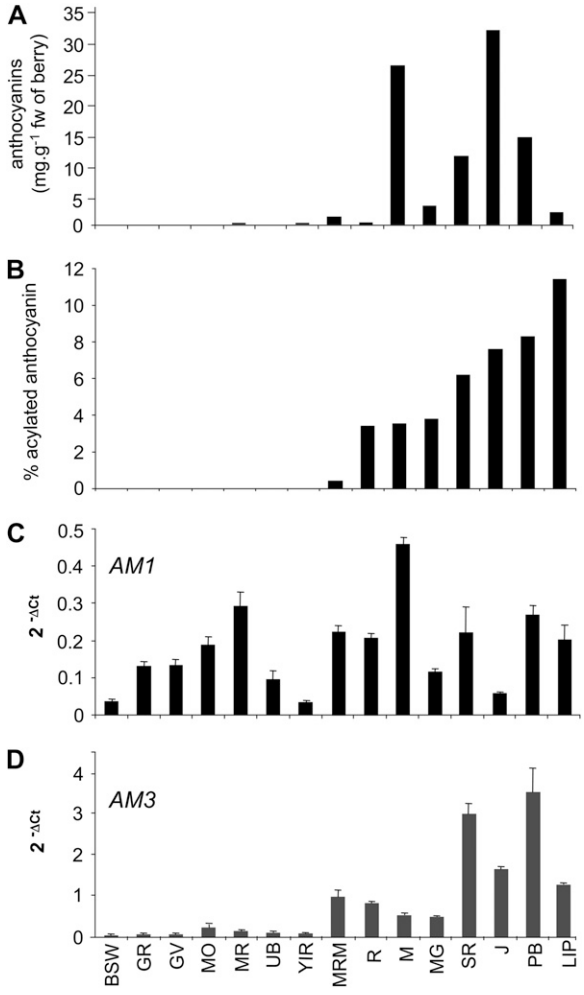

Figure 6. A, Anthocyanin content of mature berries from different cultivars. fw, Fresh weight. B, Acylated anthocyanin (expressed as percentage of total anthocyanin) in mature berries from different cultivars. C and D, Quantitative real-time PCR expression profiling of *AM1* (C) and *AM3* (D) in mature berries obtained from different cultivars. Gene expression was normalized with *VvEF1α*. All data are means of three replicates with error bars indicating SD. Cultivar names are as follows: BSW, Buckland Sweet Water; GR, Grec Rouge; GV, Goher Valtozo; MO, Muscat Ottonel; MR, Moscatel Rosado; UB, Ugni Blanc; YIR, Yai Izioum Rosovy; MRM, Muscat Rouge de Madeire; R, Rousaïtis; M, Molinara; MG, Molinera Gorda; SR, Sensit Rouge; J, Joubertin; PB, Petit Boushet; and LIP, Lledoner Pelut.

(Marinova et al., 2007). An ATP-dependent uptake of C3G by TT12-containing vesicles was observed (Supplemental Fig. S3). Using M3G or the acylated anthocyanin mixture as substrate, no transport activity could be measured with TT12-containing vesicles (Supplemental Fig. S3). The results obtained with vesicles expressing AM1, AM3, and TT12 in the uptake of different substrates, summarized in Table I, indicate that anthoMATEs mediate specifically acylated anthocyanin transport in vitro. To elucidate the type of energization mechanism, vanadate, a P-type and ABC pump inhibitor, and NH_4Cl, a reagent affecting ΔpH, were used in the transport experiments with acylated anthocyanin substrate. None of the treatments altered the level of substrate bound to empty vector-derived vesicles (Table II). The addition of NH_4Cl resulted in a strong decrease in the uptake of substrate, while vanadate had no observed effect, meaning that the uptake of acylated anthocyanins by anthoMATE proteins depends on a proton gradient (Table II). These data demonstrated that AM1 and AM3 act in vitro as vacuolar H^+-dependent acylated anthocyanin transporters.

DISCUSSION

MATE Transporters in Grapevine

The access to the whole genome sequence of grapevine (Jaillon et al., 2007) has accelerated the identification of genes underlying traits of interest in grapevine by allowing a candidate gene approach. Our work demonstrates the biochemical function of two MATE proteins involved specifically in vacuolar transport of acylated anthocyanins. The deduced amino acid sequences indicate that the AM1 and AM3 proteins have a high degree of similarity with TT12, an Arabidopsis proanthocyanidin precursor MATE transporter, and with MTP77, a tomato putative anthocyanin MATE transporter, including five conserved regions. The anthoMATEs share similar membrane topologies with the typical secondary structure of MATE-type transporters (Omote et al., 2006). Finally, anthoMATEs share the same energization mechanism with TT12. Taken together, our data provide evidence for the hypothesis formulated by Marinova et al. (2007) that homologs of the seed-specific Arabidopsis TT12 are responsible for vacuolar anthocyanin transport in other plant parts.

In addition to anthoMATEs, we revealed a large number of virtual MATE proteins (65) close to those reported in Arabidopsis (Omote et al., 2006). Plants have a large number of MATE proteins per species, in contrast to the relatively small number in the bacterial and animal kingdoms, suggesting that MATE proteins might play an important role in the detoxification of secondary metabolites and xenobiotics in plants (Omote et al., 2006). To date, few members of the MATE family, which are localized at the tonoplast or the plasma membrane, have been functionally characterized. Some MATEs are involved in root citrate exudation in Arabidopsis, sorghum (*Sorghum bicolor*), and barley (Durrett et al., 2007; Furukawa et al., 2007; Magalhaes et al., 2007; Liu et al., 2009). Recently, Shoji et al. (2009) demonstrated that a MATE protein is involved in nicotine vacuolar transport in tobacco (*Nicotiana tabacum*). For the transport of flavonoids in grapevine, Terrier et al. (2009) recently revealed the induction of a MATE transporter (GSVIVT00018839001) after the ectopic expression of proanthocyanidin tran-

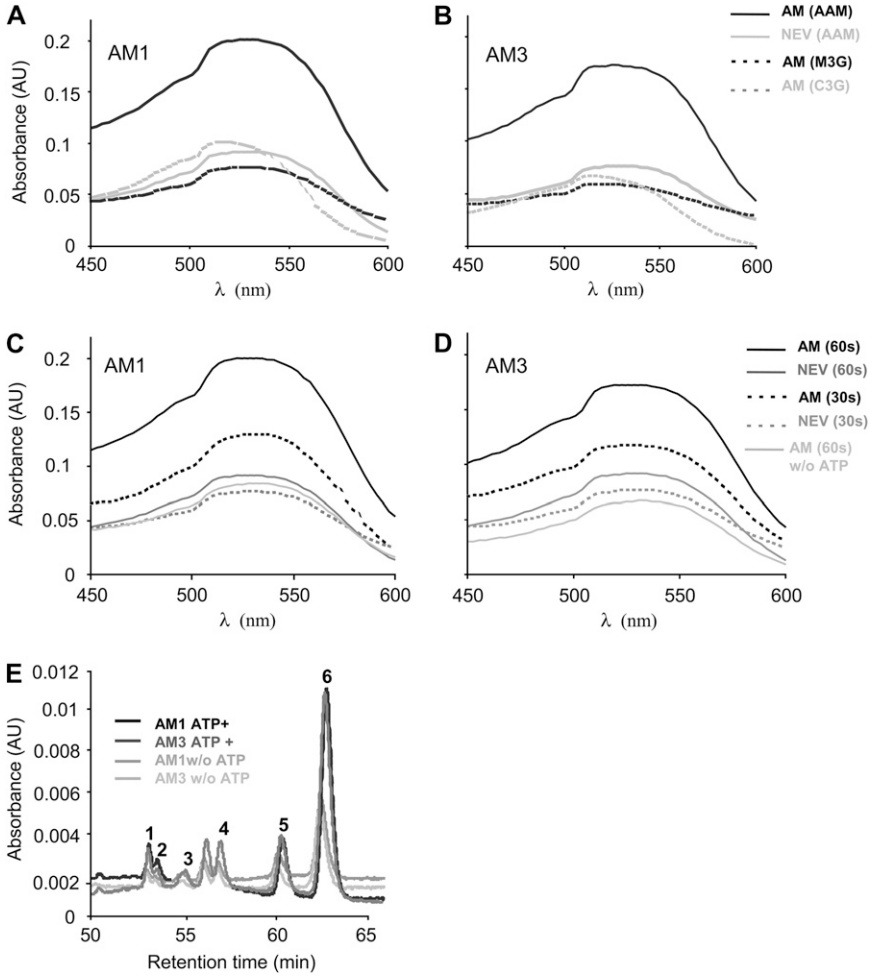

Figure 7. AM1- and AM3-mediated transport of acylated anthocyanins in yeast microsomal vesicles. A and B, Absorption scans of different substrates recovered from filters after a 1-min transport experiment in the presence of MgATP with AM1-containing vesicles (A) and AM3-contaning vesicles (B). Substrates used were as follows: acylated anthocyanin mixture (AAM; solid lines); C3G (dotted gray lines); and M3G (dotted black lines). AU, Absorbance units. C and D, Absorption scans of acylated anthocyanins washed off filters after the transport experiment with AM1-containing vesicles (C) and AM3-containing vesicles (D), representing the vesicle-associated amount of acylated anthocyanin. Transport was stopped by filtration after 30 s (dotted lines) or 60 s (solid lines). NEV, Transport experiments performed with vesicles isolated from empty vector control-transformed yeast. All transport experiments were performed in the presence of MgATP, except transport experiments after 1 min with AM-containing vesicles, which were performed with and without ATP (w/o ATP), indicated by solid gray lines. E, HPLC analysis of the acylated anthocyanins recovered from filters after a 1-min transport experiment with AM1-containing vesicles and AM3-contaning vesicles with ATP (ATP+) or without ATP (w/o ATP). Peak 1, Delphinidin 3-*p*-coumaroylglucosyl; peak 2, malvidin 3-acetylglucosyl; peak 3, cyanidin 3-*p*-coumaroylglucosyl; peak 4, petunidin 3-*p*-coumaroylglucosyl; peak 5, peonidin 3-*p*-coumaroylglucosyl; and peak 6, malvidin 3-*p*-coumaroylglucosyl.

scription factors in grapevine hairy roots. This candidate is one of the most closely related to TT12 in the phylogenetic tree presented here. Further research should confirm the important role of this MATE family in grapevine. It will be interesting to elucidate if some of these grapevine MATE transporters are also localized at the plasma membrane and mediate the transport of multiple endogenous secondary metabolites and xenobiotics.

AM1 and AM3 Exhibit Overlapping Transport Functions, But Their Expression in Mature Berries Differs among Cultivars

The high similarity found for *AM1* and *AM3* suggests that these two genes could have significant functional overlap, especially with regard to their substrate specificity. The data presented here indicate that the expression of *AM1* and *AM3* in mature berries differed among cultivars. In Arabidopsis and yeast, it was demonstrated that multicopy genes showed a rapid divergence in expression to coordinately achieve more complex control of the same genetic network (Gu et al., 2002; Blanc and Wolfe, 2004). Furthermore, Blanc and Wolfe (2004) suggested that transport activity and regulatory functions are usually found to be overduplicated for better adaptability to changing environmental conditions. For example, in maize, *ZmMRP4*, an ABC transporter sharing extensive homology with *ZmMRP3*, was detected exclusively in aleurone tissues. Both of these genes are proposed to play a role in anthocyanin sequestration (Goodman et al., 2004).

Grape berries accumulate three major types of flavonoid compounds, anthocyanins, flavonols, and flavan-3-ols, at different stages of their development (Boss et al., 1996; Downey et al., 2003). The flavan-3-ols are synthesized mainly at the green stage of berry development (Downey et al., 2003), whereas anthocyanins accumulate in berry skin during ripening only (Boss et al., 1996). By contrast, the biosynthesis of flavonols occurs at two distinct periods in grape berries, the first just after flowering and the second during ripening (Downey et al., 2003). Flavonols exist only as 3-monoglycosides in grape berries without acyl substitutions (Mattivi et al., 2006), and the flavan-3-ols, which can be acylated (galloylated; Souquet

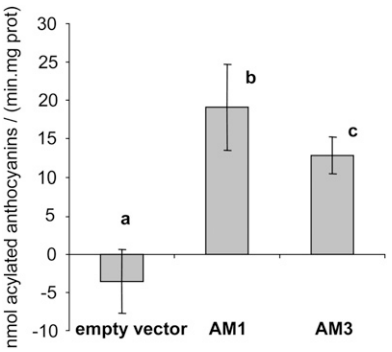

Figure 8. Quantification of MgATP-dependent uptake activity of acylated anthocyanins by AM1 and AM3. Bars show mean values of the difference between the experiments with or without the addition of MgATP ± confidence interval at 0.95. Values shown are averages of eight transport experiments performed with independent vesicle preparations. Bars associated with the same letter indicate that there are no significant differences ($P > 0.05$) by Student's *t* test.

et al., 1996), are accumulated only during the first part of berry development when anthoMATEs are not expressed. Thus, among these different flavonoid compounds, anthocyanins are the only acylated flavonoids synthesized during the induction of anthoMATEs. The biosynthetic pathways of these flavonoids are probably controlled specifically, although the regulatory network remains unclear. Moreover, in grapevine, redundancy in flavonoid structural genes has already been observed (Velasco et al., 2007). For some of them, chalcone synthase, chalcone isomerase, and flavonoid-3-hydroxylase enzymes, a divergence in gene expression has been shown, suggesting that transcription of multicopy genes could be specific for the biosynthesis of anthocyanins, flavonols, and flavan-3-ols (Castellarin et al., 2006; Jeong et al., 2008). Indeed, in grapevine hairy roots overexpressing *VlmybA1* (Cutanda-Perez et al., 2009), only *AM3* but not *AM1* was induced in this colored tissue, suggesting that *AM1* might be under the control of another transcription factor (C. Gomez, unpublished data). This finding suggests differential regulation and/or functional roles of AM1 and AM3. Recently, Deluc et al. (2008) identified the transcription factor VvMYB5b and postulated that VvMYB5b acts with VvMYBA1 and VvMYBA2 to regulate anthocyanin biosynthesis in a coordinated manner in grape berries. AM1 and AM3 exhibit at least partially overlapping transport functions, which is supported by our in vitro findings. Along this line, AM3 could be a "safety valve" that ensures vacuolar sequestration of acylated anthocyanins in situations where metabolic flux toward this class of compounds is maximized, while AM1 is the more constitutive, base-level twin. To determine whether AM1 and AM3 transport the same or structurally different substrates in planta would require a mutational or knockdown approach coupled to metabolic fingerprinting.

New Insights on the Anthocyanin Biosynthetic Pathway in Grapevine

AM1 and AM3 mediate the transport of anthocyanin-acylglucosides, while anthocyanin-glucosides were not transported under our experimental conditions. This suggests that the acyl conjugation is essential for the uptake of anthocyanin by anthoMATEs. Transport studies with isolated vacuoles from parsley (*Petroselinum crispum*) and carrot earlier indicated that the acyl residues attached to flavonoids are important determinants of substrate specificity (Matern et al., 1986; Hopp and Seitz, 1987). Moreover, pH-driven conformational changes of the malonylglucosides were suggested to be responsible for vacuolar trapping of flavonoids in parsley (Matern et al., 1986). Our data support the hypothesis that acylation reactions may be critical to provide the correct substrates for vacuolar deposition. This would imply that the acylation reactions take place prior to transport, and consequently in the cytosol.

Until now, to our knowledge, no anthocyanin acyltransferase has been identified in grapevine. It remains unclear if the methylation and the acylation take place in a chronological manner into the anthocyanin pathway. No evidence has been provided whether the enzymes are localized in the cytoplasm or inside the vacuole. Research in other plants revealed that the modification of anthocyanins is family or species dependent (Tanaka et al., 2008). Two types of acyltransferases could be involved in anthocyanin acylation: the BAHD acyltransferases, belonging to a large family of acyl CoA-utilizing enzymes, would be localized to the cytosol (Fujiwara et al., 1998; Yonekura-Sakakibara et al., 2000; D'Auria, 2006), and the SCPL family, whose members are acyl Glc dependent, would be localized to the vacuole (Noda et al., 2007; Tanaka et al., 2008). Our results suggest that anthocyanin acyltransferases in grape berry could be part of the BAHD family.

Different forms of anthocyanin accumulation have been observed as intravacuolar bodies and are referred as anthocyanin vacuolar inclusions (AVIs) in different plants. In flower coloration, AVIs showed a major influence on flower color by enhancing intensity and blueness by concentrating anthocyanins above

Table I. *Uptake of different substrates into vesicles isolated from AM1-, AM3-, or TT12-transformed yeast*

AAM, Acylated anthocyanin mixture. The presence and absence of transport activity with the corresponding substrate is indicated by + and −, respectively.

Protein	Substrate Uptake		
	C3G	M3G	AAM
AM1	−	−	+
AM3	−	−	+
TT12	+[a]	−	−

[a]From this work and Marinova et al. (2007).

Table II. *Effects of inhibitors on the uptake of acylated anthocyanin substrate*

The uptake in the absence of inhibitors was set to 100% (for AM1). All experiments were performed in the presence of MgATP. Values were means of *n* independent experiments with four independent vesicle preparations.

Condition	Acylated Anthocyanin Uptake		
	NEV	AM1	AM3
		% of control	
None	19 (n = 10)	100 (n = 10)	67 (n = 8)
Vanadate (1 mM)	22 ± 3 (n = 4)	75 ± 3 (n = 4)	102 ± 2 (n = 4)
NH_4Cl (5 mM)	20 ± 3 (n = 4)	15 ± 5 (n = 4)	21 ± 5 (n = 4)

levels that would be impossible in vacuolar solution (Markham et al., 2000). In grapevine cell suspension, Conn et al. (2003) suggested that AVIs selectively bind acylated anthocyanins. In order to increase the level of more stable anthocyanins, the induction of AVIs may be an interesting approach. It appears that acylation may contribute to AVI formation in plants. Therefore, vacuolar acylated anthocyanin transporter might play an important role. In grapevine, it will be important to determine if a direct relation between AVI formation and anthoMATEs exists. Nevertheless, no associated boundary membrane in AVIs has yet been demonstrated.

Anthocyanin Transport in Grape Berries May Involve Different Transport Mechanisms

AnthoMATE proteins mediate specifically acylated anthocyanin transport in vitro. This suggests that other mechanisms should be involved in the transport of the nonacylated anthocyanins predominating in grape berries. Whether MRP transporters and MATE transporters are involved in anthocyanin transport has been a matter of debate. For MATE transporters, our work indicates that acyl residues are important determinants for transport. In vitro, TT12 transported C3G in an ATP-dependent and uncoupler-sensitive manner but not the aglycones cyanidin or epicatechin (Marinova et al., 2007). In vivo, Marinova et al. (2007) proposed that TT12 transports proanthocyanidin precursors that are likely glycosylated flavan-3-ols. Omote et al. (2006) speculated that the existence of many plant MATEs might correspond to the transport of large numbers of secondary metabolites. Taken together, a specificity of MATE transporters might be speculated or suggested in flavonoid transport.

For MRP transporters, their specificity is less reported. In grapevine hairy roots expressing ectopically *VlmybA1-2*, a high-throughput (but nonexhaustive) transcriptomic screening did not reveal genes encoding for proteins with a structure highly similar to MRP proteins (Cutanda-Perez et al., 2009). In Arabidopsis knockout mutants, some MRPs have been identified, but none of them have resulted in flavonoidless phenotypes. AtMRP transporters exhibited an extensive range of substrates (Lu et al., 1997; Liu et al., 2001). In addition, in maize, Goodman et al. (2004) reported that the loss of ZmMRP3 function induced a mislocalization of anthocyanins, with no alteration in the anthocyanin species produced, and that the loss of ZmMRP3 function throughout the plant may negatively affect viability. All of these data suggest multiple biological roles for this family of transporters. It will be particularly important to know whether the anthocyanin transport is handled in a nonspecific manner with MRPs and in a specific manner with MATEs.

In this study, AM1::GFP and AM3::GFP protein fusions were localized at the tonoplast and in membrane structures attached to the nucleus of grapevine hairy root epidermal cells. Recently, in Arabidopsis seedlings, anthocyanins were localized in cytoplasmic structures that resemble ER bodies (Poustka et al., 2007), and in tapetum cells, flavonoids were localized in the ER network and in ER-derived tapetosomes (Hsieh and Huang, 2007). In addition, Hsieh and Huang (2007) reported that in the tapetum cells of the Arabidopsis *tt12* mutant, the flavonoids were present in the cytosol and were not associated with tapetosomes, suggesting that TT12 may be also implicated in the filling of ER-derived tapetosomes and thus localized elsewhere than on the vacuolar membrane. In Marinova et al. (2007), TT12 was found to be localized exclusively to the tonoplast; however, its in vivo localization was performed on organs that do not accumulate flavonoids. Whether anthoMATE proteins are localized exclusively on the vacuolar membrane or also on the ER and in the prevacuolar compartment membrane is unclear at this time and will be further investigated. The possibility that in grape berries the lumen of the ER provides the initial site for anthocyanin accumulation suggests that the two models reviewed by Grotewold and Davies (2008), the VT and the LT model, may be involved in grape berries. In relation to the LT model, genetic evidence in maize, petunia, and Arabidopsis suggests that a specific GST is necessary for the correct anthocyanin accumulation inside the vacuole (Marrs et al., 1995; Alfenito et al., 1998; Kitamura et al., 2004). The interaction between anthocyanins and GST has not been clearly characterized. According to the LT model, the GST might escort the anthocyanin to the tonoplast. It will be important to address the question of whether a relation between the grape berry GST (Conn et al., 2008) and anthoMATEs exists.

In conclusion, this study reports specific transport of acylated anthocyanins mediated by vacuolar anthoMATE transporters. We suggest that the MATE proteins identified here act as acylation-dependent anthocyanin transporters in grape berry. The existence of other transport mechanisms has to be elucidated, and the characterization of their in vivo role would supply more evidence about a hypothetical relationship between the transport mechanism and the anthocyanin composition. However, it is important to note that the anthocyanin composition is different in each plant species. It will be interesting to investigate how the overall anthocyanin structures biosynthesized in one species reflect the transport mechanisms used and if the transport mechanism used is more species specific or anthocyanin structure specific.

MATERIALS AND METHODS

Chemicals and Pigment Extraction

M3G and C3G were purchased from Extrasynthese. All other chemicals were from Sigma-Aldrich.

The mixture of acylated anthocyanins was isolated from grapevine (*Vitis vinifera* 'Syrah') berry. At first, an anthocyanin extract was prepared from grape skin powder by extraction with methanol:water:HCl (30:70:0.2, v/v/v) twice for 3 h at room temperature. Then, after concentration of this extract under vacuum, HPLC separation was performed by means of a Gilson system equipped with a reverse-phase Microsorb C18 column (100 Å, 5 μm, 220 × 22.4 mm i.d.). Elution was with solvent A (water:chlorhydric acid, 99.8:0.2, v/v) and solvent B (acetonitrile:water:chlorhydric acid, 80:19.8:0.2, v/v/v) with a 10 mL min^{-1} flow rate, linear gradients from 18% to 21% B in 10 min, from 21% to 30% B in 10 min, and from 30% to 80% B in 2 min, followed by washing and reequilibrating of the column. Its composition was determined by HPLC analysis as described by Fournand et al. (2006). This fraction, named acylated anthocyanin mixture, contained 6.6% M3G, 6.2% malvidin 3-*O*-acetylglucoside, 3.4% delphinidin 3-*O*-*p*-coumaroylglucoside, 2% cyanidin 3-*O*-*p*-coumaroylglucoside, 6.7% petunidin 3-*O*-*p*-coumaroylglucoside, 14.7% peonidin 3-*O*-*p*-coumaroylglucoside, and 60.4% malvidin 3-*O*-*p*-coumaroylglucoside.

For uptake experiments, M3G, C3G, and the acylated anthocyanin mixture were dissolved as 10 mM stock in 10% methanol and 0.1% HCl.

Plant Material

Roots, shoots, leaves, and berries were harvested from grapevine plants (Syrah) grown in the SupAgro-INRA vineyard in Montpellier, France. Young leaves were from the third rank, counted from the apex, with mean weight of 0.3 g per leaf. Old leaves were fully expanded leaves with mean weight of 2.8 g per leaf. Berries were collected at nine developmental stages as described previously (Terrier et al., 2005).

For the expression analysis, 15 genotypes were selected to maximize the phenotypic variation for the anthocyanin berry content (Supplemental Table S1). Berries were sorted on a sodium chloride density gradient in order to compare berries at the same level of maturity (density of 100–120 g L^{-1}). All collected samples were quickly frozen in liquid nitrogen, ground to a fine powder with a Dangoumau blender, and stored at –80°C until use. Anthocyanins were analyzed by HPLC according to Fournand et al. (2006).

Gene Expression Analysis

RNA was extracted from 200 mg of starting tissue using the RNeasy Plant Mini Kit (Qiagen) following the manufacturer's protocol. RNA was quantified with Ribogreen (Molecular Probes), and reverse transcription was performed from each sample from 500 ng of purified RNA using the SuperScript II RT Kit (Life Technologies). PCR amplification was performed from 125 ng of cDNA using the SYBR Green PCR Master Mix (Perkin-Elmer Applied Biosystems) with the 7300 Sequence Detection System (Applied Biosystems). Gene transcripts were quantified upon normalization to *VvEF1α* as an internal standard. Results are reported as $2^{-\Delta CT}$, where ΔCT is the number of PCR cycles required for the log phase of amplification for the experimental gene minus the same measure for *VvEF1* (Livak and Schmittgen, 2001). All biological samples were tested in triplicate, and SE values of means were calculated using standard statistical methods. Primers used for amplification were as follows: *AM1* forward, 5′-TGCTTTTGTGATTTTGTTAGAGG-3′, and *AM1* reverse, 5′-CCCTTCCCCGATTGAGAGTA-3′; *AM3* forward, 5′-GCAAACAACAGAGAGGATGC-3′, and *AM3* reverse, 5′-AGACCTCGACAATGATCTTAC-3′. All primers pairs were determined to have equal amplification efficiency, and the PCR products were resolved by electrophoresis. Specific annealing of the oligonucleotides was controlled by dissociation kinetics performed at the end of each PCR run.

Phylogenetic and Sequence Analyses

Grapevine sequences were recovered and annotated by the Genoscope genome browser (http://www.genoscope.cns.fr/vitis/; data obtained from the 8-fold coverage of the genome). Database searches for homologous sequences were performed on the BLAST server (http://www.ncbi.nlm.nih.gov/blast/Blast.cgi). Multiple sequence alignment was performed with ClustalW alignment (http://www.ebi.ac.uk/Tools/clustalw2/index.html). Phylogenetic analysis was performed using Protml of the Phylip package (http://evolution.genetics.washington.edu/phylip.html) and edited with Dissimilarity Analysis and Representation for Windows (DARwin) software (http://darwin.cirad.fr/darwin). Information on the transporter domain was obtained from the Pfam database (http://pfam.sanger.ac.uk/). Transmembrane regions were predicted by the HMMTOP program (http://www.enzim.hu/hmmtop/index.html).

Subcellular Localization and Confocal Scanning Microscopy

The AM1::GFP and AM3::GFP fusions were obtained by Gateway cloning strategy (Invitrogen). The stop-codon-less *AM1* and *AM3* cDNAs were amplified using high-fidelity Taq Polymerase (Advantage-HF2 PCR Kit; Clontech) according to the manufacturer's instructions. The following primers were used: *AM1* forward, 5′-CACCATGGAGACGCCGCTGCTCAACAG-3′, and *AM1* reverse, 5′-GACATCATCACTCGTCTTCTT-3′; *AM3* forward, 5′-CACCATGGAGACACCGCTGCTCAAGAGC-3′, and *AM3* reverse, 5′-TACATCATCGGCTTCAATCC-3′. The resulting PCR products were transferred into pENTR/D-TOPO vector (Invitrogen) and subsequently into pH7FWG2 (Karimi et al., 2002) by TOPO and LR clonase reactions according to the manufacturer's instructions.

Subcellular localization of AM1::GFP and AM3::GFP fusions was investigated after stable transformation of root lines of grapevine (cv Maccabeu). Induction and culture of transformed root lines were performed as described by Torregrosa and Bouquet (1997) with the following modifications: (1) *Agrobacterium rhizogenes* A4 strain was the undisarmed vector; (2) bacterial cultures were grown on semisolid MGL/B medium (5 g L^{-1} tryptone, 5 g L^{-1} mannitol, 2.5 g L^{-1} yeast extract, 1 g L^{-1} Glu, 250 mg L^{-1} K_2HPO_4, 100 mg L^{-1} NaCl, 100 mg L^{-1} $MgSO_4.7H_2O$, and 5 μg L^{-1} biotin at pH 7; Torregrosa et al., 2002) supplemented with 50 μg mL^{-1} spectinomycin and then suspended with half-strength Murashige and Skoog liquid medium with 100 μM acetosyringone (optical density at 600 nm = 0.5); and (3) extracted roots tips were cultured on LGO medium (LGO as described by Torregrosa and Bouquet [1997]) solidified with 5 g L^{-1} Phytagel (Sigma) containing 200 mg L^{-1} of both augmentin and cefotaxime (Duchefa) to prevent bacteria growth. Microscopy observations were performed after three hairy root subcultures with three independent hairy root clones arising from separated induction experiments. DNA was extracted from 100 mg of fresh tissue using the DNA Plant Mini Kit (Qiagen). Transformants were checked by PCR using the hygromycin primers 5′-GCCTGAACTCACCGCGACGTC-3′ and 5′-CAGTTTGCCAGTGATACAC-3′.

For confocal microscopy analysis, young root tips were placed in 1 μM DAPI for 10 min and then rinsed in 10 mM phosphate-buffered saline, pH 7.2, with or without 0.3 M sorbitol and mounted with the same buffer. The confocal microscope was focused on the epidermal or subepidermal cell layer. GFP was excited at 488 nm with an argon laser, and the emission was collected between 500 and 530 nm. DAPI was excited at 730 nm with a Chameleon Ultra II laser, and the emission was collected between 385 and 465 nm. The fluorescence was

detected in multitrack configuration using the Axiovert Zeiss LSM 510 META NLO multiphotonic microscope (available at the Montpellier RIO Imaging Platform; www.mri.cnrs.fr). The specificity of signal GFP was checked by spectral analysis. Images were edited using Zeiss LSM Image Browser software and assembled for figures in Adobe Photoshop 7.0.

Preparation of Yeast Vesicles and in Vitro Transport Studies

The full-length cDNAs of AM1 and AM3 were amplified from cDNA of mature berries (Syrah) using high-fidelity Taq Polymerase (Advantage-HF2 PCR kit; Clontech) according to the manufacturer's instructions. The following primers were used: AM1 forward, 5′-GCGGCCGCATGGAGACG-CCGCTGCTCAACAG-3′, and AM1 reverse, 5′-GCGGCCGCTCAGACAT-CATCACTCGTCTTCTT-3′; AM3 forward, 5′-GCGGCCGCATGGAGA-CACCGCTGCTCAAGAGC-3′, and AM3 reverse, 5′-GCGGCCGCTCATA-CATCATCGGCTTCAATCC-3′. The *Not*I restriction site, added in all of the primers, is underlined. The amplified cDNAs for AM1 and AM3 were cloned into the pGEM-T Easy vector (Promega), and the resulting plasmids were then sequenced using M13 forward and M13 reverse primers by commercial DNA sequencing service providers (GATC Biotech). PCR products of *AM1* and *AM3* were cloned into the *Not*I site of the plasmid pNEV-Ura (Sauer and Stolz, 1994), resulting in pNEV-AM1 and pNEV-AM3. The constructs were sequenced to verify that no mutation had been introduced. These two constructs were then used to transform the yeast strain YPH 499 (MATa URA3-52 lys2-801 ade2-101 trp1-Δ63 his3-Δ200 leu2-1) following standard procedures (Gietz and Woods, 2002). Transformants were selected on minimal synthetic dropout medium lacking uracil.

Western Blot

The isolated vesicle extracts were dissociated with SDS sample buffer containing 10% SDS and 10% mercaptoethanol and incubated in a 100°C bath for 3 min. The proteins were subjected to electrophoresis on 10% polyacrylamide gels in the presence of SDS. Western blotting of the vesicle extracts isolated was performed as described by Terrier et al. (1998). The anti-anthoMATE antibody was obtained from rabbit sera, following immunization with the peptide AALSIRVSNELGYGHPRAAK. Antibody was purchased from Proteogenix.

Yeast membrane vesicles for in vitro transport studies were isolated essentially as described by Tommasini et al. (1996) with the modifications reported by Klein et al. (2002) without the addition of bovine serum albumin into the vesicle buffer. Protein concentration was determined by the method of Bradford (1976) using bovine serum albumin as the standard. Tightness of the vesicle fractions isolated from yeast transformants was evaluated by fluorescence quenching of the dye ACMA. Vesicle extracts (300 μg) were added to the assay cuvette (2 mL final) containing 2 μM ACMA, 0.4 M glycerol, 6 mM $MgSO_4$, 1 mM dithiothreitol, 100 mM KCl, and 20 mM Tris-MES, pH 7.4. The cuvette was stirred and maintained at 30°C. MgATP (5 mM) was added, and fluorescence intensities of the probes were simultaneously measured with an SLM Amico-Bowman spectrofluorimeter. ACMA signal was acquired at 480 nm after excitation at 415 nm. The references for the signals were obtained by collapsing the pH gradient by addition of 25 mM $(NH_4)_2SO_4$.

Uptake experiments to study the transport of anthocyanin substrates into membrane vesicles were performed using the rapid filtration technique with nitrocellulose filters (0.45-mm pore size; Millipore) as described by Marinova et al. (2007). Immediately after the experiment, filter-bound anthocyanins were dissolved by adding 500 μL of 50% methanol and 0.1% HCl. Anthocyanin content eluted from the filters was analyzed by absorption spectra scans between 450 and 600 nm with the SAFAS monaco UV mc^2 spectrophotometer. HPLC analysis was performed according to Fournand et al. (2006) after the injection of 5 μL of the anthocyanin solutions eluted from the filters.

Sequence data from this article have been deposited with the GenBank/EMBL data libraries under accession numbers FJ264202 (AM1) and FJ264203 (AM3).

Supplemental Data

The following materials are available in the online version of this article.

Supplemental Figure S1. Subcellular localization of anthoMATE protein after transient expression in onion bulb epidermal cells (A) and after stable expression in grapevine (B).

Supplemental Figure S2. Analysis of vesicle fractions isolated from yeast transformants.

Supplemental Figure S3. TT12 transport activity toward M3G, C3G, and acylated anthocyanin mixture substrates.

Supplemental Table S1. Anthocyanin profiles of mature berries from a set of 15 grapevine cultivars used for expression analysis.

ACKNOWLEDGMENTS

We especially thank G. Conejero for her helpful assistance for confocal microscopy. The A4 strain was introduced from the Centre Français des Bacteries Phytopathogènes d'Angers (http://www-intranet.angers.inra.fr). We thank C. Romieu for providing Gateway pH7FWG2-compatible cloning vector, F.X. Sauvage for technical support with western blotting, and I. Gil and G. Lopez for their assistance in the handling of the in vitro vegetal material.

Received January 13, 2009; accepted March 16, 2009; published March 18, 2009.

LITERATURE CITED

Ageorges A, Fernandez L, Vialet S, Merdinoglu D, Terrier N, Romieu C (2006) Four specific isogenes of the anthocyanin metabolic pathway are systematically co-expressed with the red colour of grape berries. Plant Sci **170:** 372–383

Alfenito MR, Souer E, Goodman CD, Buell R, Mol J, Koes R, Walbot V (1998) Functional complementation of anthocyanin sequestration in the vacuole by widely divergent glutathione S-transferases. Plant Cell **10:** 1135–1149

Archetti M (2000) The origin of autumn colours by coevolution. J Theor Biol **205:** 625–630

Blanc G, Wolfe KH (2004) Functional divergence of duplicated genes formed by polyploidy during *Arabidopsis* evolution. Plant Cell **16:** 1679–1691

Boss PK, Davies C, Robinson SP (1996) Analysis of the expression of anthocyanin pathway genes in developing *Vitis vinifera* L. cv Shiraz grape berries and the implications for pathway regulation. Plant Physiol **111:** 1059–1066

Bradford MM (1976) Rapid and sensitive method for the quantitation of microgram quantities of protein utilizing the principle of protein-dye binding. Anal Biochem **72:** 248–254

Braidot E, Petrussa E, Bertolini A, Peresson C, Ermacora P, Loi N, Terdoslavich M, Passamonti S, Macri F, Vianello A (2008) Evidence for a putative flavonoid translocator similar to mammalian bilitranslocase in grape berries (*Vitis vinifera* L.) during ripening. Planta **228:** 203–213

Broun P (2005) Transcriptional control of flavonoid biosynthesis: a complex network of conserved regulators involved in multiple aspects of differentiation in Arabidopsis. Curr Opin Plant Biol **8:** 272–279

Castellarin SD, Di Gaspero G, Marconi R, Nonis A, Peterlunger E, Paillard S, Adam-Blondon AF, Testolin R (2006) Colour variation in red grapevines (*Vitis vinifera* L.): genomic organisation, expression of flavonoid 3′-hydroxylase, flavonoid 3′,5′-hydroxylase genes and related metabolite profiling of red cyanidin-/blue delphinidin-based anthocyanins in berry skin. BMC Genomics **7:** 12

Cheynier V, Duenas-Paton M, Salas E, Maury C, Souquet JM, Sarni-Manchado P, Fulcrand H (2006) Structure and properties of wine pigments and tannins. Am J Enol Vitic **57:** 298–305

Conn S, Curtin C, Bezier A, Franco C, Zhang W (2008) Purification, molecular cloning, and characterization of glutathione S-transferases (GSTs) from pigmented *Vitis vinifera* L. cell suspension cultures as putative anthocyanin transport proteins. J Exp Bot **59:** 3621–3634

Conn S, Zhang W, Franco C (2003) Anthocyanic vacuolar inclusions (AVIs) selectively bind acylated anthocyanins in *Vitis vinifera* L. (grapevine) suspension culture. Biotechnol Lett **25:** 835–839

Cutanda-Perez MC, Ageorges A, Gomez C, Vialet S, Terrier N, Romieu C, Torregrosa L (2009) Ectopic expression of *VlmybA1* in grapevine activates a narrow set of genes involved in anthocyanin synthesis and transport. Plant Mol Biol **69:** 633–648

Czempinski K, Frachisse JM, Maurel C, Barbier-Brygoo H, Mueller-Roeber B (2002) Vacuolar membrane localization of the *Arabidopsis* 'two-pore' K^+ channel KCO1. Plant J **29:** 809–820

Dangles O, Saito N, Brouillard R (1993) Anthocyanin intramolecular copigment effect. Phytochemistry **34:** 119–124

D'Auria JC (2006) Acyltransferases in plants: a good time to be BAHD. Curr Opin Plant Biol **9:** 331–340

Debeaujon I, Peeters AJM, Leon-Kloosterziel KM, Koornneef M (2001) The TRANSPARENT TESTA 12 gene of *Arabidopsis* encodes a multidrug secondary transporter-like protein required for flavonoid sequestration in vacuoles of the seed coat endothelium. Plant Cell **13:** 853–871

Deluc L, Bogs J, Walker AR, Ferrier T, Decendit A, Merillon JM, Robinson SP, Barrieu F (2008) The transcription factor VvMYB5b contributes to the regulation of anthocyanin and proanthocyanidin biosynthesis in developing grape berries. Plant Physiol **147:** 2041–2053

Downey MO, Harvey JS, Robinson SP (2003) Synthesis of flavonols and expression of flavonol synthase genes in the developing grape berries of Shiraz and Chardonnay (*Vitis vinifera* L.). Aust J Grape Wine Res **9:** 110–121

Durrett TP, Gassmann W, Rogers EE (2007) The FRD3-mediated efflux of citrate into the root vasculature is necessary for efficient iron translocation. Plant Physiol **144:** 197–205

Fournand D, Vicens A, Sidhoum L, Souquet JM, Moutounet M, Cheynier V (2006) Accumulation and extractability of grape skin tannins and anthocyanins at different advanced physiological stages. J Agric Food Chem **54:** 7331–7338

Fujiwara H, Tanaka Y, Yonekura-Sakakibara K, Fukuchi-Mizutani M, Nakao M, Fukui Y, Yamaguchi M, Ashikari T, Kusumi T (1998) cDNA cloning, gene expression and subcellular localization of anthocyanin 5-aromatic acyltransferase from *Gentiana triflora*. Plant J **16:** 421–431

Furukawa J, Yamaji N, Wang H, Mitani N, Murata Y, Sato K, Katsuhara M, Takeda K, Ma JF (2007) An aluminum-activated citrate transporter in barley. Plant Cell Physiol **48:** 1081–1091

Gietz RD, Woods RA (2002) Transformation of yeast by lithium acetate/single-stranded carrier DNA/polyethylene glycol method. Methods Enzymol **350:** 87–96

Goodman CD, Casati P, Walbot V (2004) A multidrug resistance-associated protein involved in anthocyanin transport in *Zea mays*. Plant Cell **16:** 1812–1826

Grotewold E, Chamberlin M, Snook M, Siame B, Butler L, Swenson J, Maddock S, Clair GS, Bowen B (1998) Engineering secondary metabolism in maize cells by ectopic expression of transcription factors. Plant Cell **10:** 721–740

Grotewold E, Davies K (2008) Trafficking and sequestration of anthocyanins. Nat Prod Commun **3:** 1251–1258

Gu ZL, Nicolae D, Lu HHS, Li WH (2002) Rapid divergence in expression between duplicate genes inferred from microarray data. Trends Genet **18:** 609–613

Harborne JB, Williams CA (2000) Advances in flavonoid research since 1992. Phytochemistry **55:** 481–504

Hopp W, Seitz HU (1987) The uptake of acylated anthocyanin into isolated vacuoles from a cell suspension culture of *Daucus carota*. Planta **170:** 74–85

Hsieh K, Huang AHC (2007) Tapetosomes in *Brassica* tapetum accumulate endoplasmic reticulum-derived flavonoids and alkanes for delivery to the pollen surface. Plant Cell **19:** 582–596

Jaillon O, Aury JM, Noel B, Policriti A, Clepet C, Casagrande A, Choisne N, Aubourg S, Vitulo N, Jubin C, et al (2007) The grapevine genome sequence suggests ancestral hexaploidization in major angiosperm phyla. Nature **449:** 463–467

Jeong ST, Goto-Yamamoto N, Hashizume K, Esaka M (2008) Expression of multi-copy flavonoid pathway genes coincides with anthocyanin, flavonol and flavan-3-ol accumulation of grapevine. Vitis **47:** 135–140

Karimi M, Inze D, Depicker A (2002) GATEWAY vectors for Agrobacterium-mediated plant transformation. Trends Plant Sci **7:** 193–195

Kitamura S, Shikazono N, Tanaka A (2004) TRANSPARENT TESTA 19 is involved in the accumulation of both anthocyanins and proanthocyanidins in Arabidopsis. Plant J **37:** 104–114

Klein M, Burla B, Martinoia E (2006) The multidrug resistance-associated protein (MRP/ABCC) subfamily of ATP-binding cassette transporters in plants. FEBS Lett **580:** 1112–1122

Klein M, Mamnun YM, Eggmann T, Schuller C, Wolfger H, Martinoia E, Kuchler K (2002) The ATP-binding cassette (ABC) transporter Bpt1p mediates vacuolar sequestration of glutathione conjugates in yeast. FEBS Lett **520:** 63–67

Klein M, Weissenbock G, Dufaud A, Gaillard C, Kreuz K, Martinoia E (1996) Different energization mechanisms drive the vacuolar uptake of a flavonoid glucoside and a herbicide glucoside. J Biol Chem **271:** 29666–29671

Liu GS, Sanchez-Fernandez R, Li ZS, Rea PA (2001) Enhanced multispecificity of Arabidopsis vacuolar multidrug resistance-associated protein-type ATP-binding cassette transporter, AtMRP2. J Biol Chem **276:** 8648–8656

Liu J, Magalhaes JV, Shaff J, Kochian LV (2009) Aluminum-activated citrate and malate transporters from the MATE and ALMT families function independently to confer Arabidopsis aluminum tolerance. Plant J **57:** 389–399

Livak KJ, Schmittgen TD (2001) Analysis of relative gene expression data using real-time quantitative PCR and the $2^{-\Delta CT}$ method. Methods **25:** 402–408

Lu YP, Li ZS, Drozdowicz YM, Hortensteiner S, Martinoia E, Rea PA (1998) AtMRP2, an *Arabidopsis* ATP binding cassette transporter able to transport glutathione S-conjugates and chlorophyll catabolites: functional comparisons with AtMRP1. Plant Cell **10:** 267–282

Lu YP, Li ZS, Rea PA (1997) AtMRP1 gene of Arabidopsis encodes a glutathione S-conjugate pump: isolation and functional definition of a plant ATP-binding cassette transporter gene. Proc Natl Acad Sci USA **94:** 8243–8248

Magalhaes JV, Liu J, Guimaraes CT, Lana UGP, Alves VMC, Wang YH, Schaffert RE, Hoekenga OA, Pineros MA, Shaff JE, et al (2007) A gene in the multidrug and toxic compound extrusion (MATE) family confers aluminum tolerance in sorghum. Nat Genet **39:** 1156–1161

Manetas Y (2006) Why some leaves are anthocyanic and why most anthocyanic leaves are red? Flora **201:** 163–177

Marinova K, Pourcel L, Weder B, Schwarz M, Barron D, Routaboul JM, Debeaujon I, Klein M (2007) The *Arabidopsis* MATE transporter TT12 acts as a vacuolar flavonoid/H^+-antiporter active in proanthocyanidin-accumulating cells of the seed coat. Plant Cell **19:** 2023–2038

Markham KR, Gould KS, Winefield CS, Mitchell KA, Bloor SJ, Boase MR (2000) Anthocyanic vacuolar inclusions: their nature and significance in flower colouration. Phytochemistry **55:** 327–336

Marrs KA, Alfenito MR, Lloyd AM, Walbot V (1995) A glutathione-S-transferase involved in vacuolar transfer encoded by the maize gene Bronze-2. Nature **375:** 397–400

Martinoia E, Maeshima M, Neuhaus HE (2007) Vacuolar transporters and their essential role in plant metabolism. J Exp Bot **58:** 83–102

Matern U, Reichenbach C, Heller W (1986) Efficient uptake of flavonoids into parsley (*Petroselinum hortense*) vacuoles requires acylated glycosides. Planta **167:** 183–189

Mathews H, Clendennen SK, Caldwell CG, Liu XL, Connors K, Matheis N, Schuster DK, Menasco DJ, Wagoner W, Lightner J, et al (2003) Activation tagging in tomato identifies a transcriptional regulator of anthocyanin biosynthesis, modification, and transport. Plant Cell **15:** 1689–1703

Mattivi F, Guzzon R, Vrhovsek U, Stefanini M, Velasco R (2006) Metabolite profiling of grape: flavonols and anthocyanins. J Agric Food Chem **54:** 7692–7702

Noda N, Higaki T, Sano T, Kazuma K, Sasaki T, Hasezawa S, Suzuki M (2007) The subcellular localization and substrate specificity of 1-O-acylglucose dependent anthocyanin acyltransferase from blue petal of butterfly pea (*Clitoria ternatea*). Plant Cell Physiol (Suppl) **48:** S222

Omote H, Hiasa M, Matsumoto T, Otsuka M, Moriyama Y (2006) The MATE proteins as fundamental transporters of metabolic and xenobiotic organic cations. Trends Pharmacol Sci **27:** 587–593

Poustka F, Irani NG, Feller A, Lu Y, Pourcel L, Frame K, Grotewold E (2007) A trafficking pathway for anthocyanins overlaps with the endoplasmic reticulum-to-vacuole protein-sorting route in Arabidopsis and contributes to the formation of vacuolar inclusions. Plant Physiol **145:** 1323–1335

Roggero JP, Larice JL, Rocheville-Divorne C, Archier P, Cohen S (1988) Composition anthocyanique des cépages: essai de classification par

analyse en composantes principales et analyse factorielle discriminante. Cahiers Scientifiques RFOE **112:** 277–284

Saslowsky D, Winkel-Shirley B (2001) Localization of flavonoid enzymes in Arabidopsis roots. Plant J **27:** 37–48

Sauer N, Stolz J (1994) SUC1 and SUC2: two sucrose transporters from *Arabidopsis thaliana*; expression and characterization in baker's yeast and identification of the histidine-tagged protein. Plant J **6:** 67–77

Shoji T, Inai K, Yazaki Y, Sato Y, Takase H, Shitan N, Yazaki K, Goto Y, Toyooka K, Matsuoka K, et al (2009) Multidrug and toxic compound extrusion-type transporters implicated in vacuolar sequestration of nicotine in tobacco roots. Plant Physiol **149:** 708–718

Souquet JM, Cheynier V, Brossaud F, Moutounet M (1996) Polymeric proanthocyanidins from grape skins. Phytochemistry **43:** 509–512

Tanaka Y, Sasaki N, Ohmiya A (2008) Biosynthesis of plant pigments: anthocyanins, betalains and carotenoids. Plant J **54:** 733–749

Terrier N, Deguilloux C, Sauvage FX, Martinoia E, Romieu C (1998) Proton pumps and anion transport in *Vitis vinifera*: the inorganic pyrophosphatase plays a predominant role in the energization of the tonoplast. Plant Physiol Biochem **36:** 367–377

Terrier N, Glissant D, Grimplet J, Barrieu F, Abbal P, Couture C, Ageorges A, Atanassova R, Leon C, Renaudin JP, et al (2005) Isogene specific oligo arrays reveal multifaceted changes in gene expression during grape berry (*Vitis vinifera* L.) development. Planta **222:** 832–847

Terrier N, Torregrosa L, Ageorges A, Vialet S, Verries C, Cheynier V, Romieu C (2009) Ectopic expression of VvMybPA2 promotes proanthocyanidin biosynthesis in *Vitis vinifera* L. and suggests additional targets in the pathway. Plant Physiol **149:** 1028–1041

Tommasini R, Evers R, Vogt E, Mornet C, Zaman GJR, Schinkel AH, Borst P, Martinoia E (1996) The human multidrug resistance-associated protein functionally complements the yeast cadmium resistance factor 1. Proc Natl Acad Sci USA **93:** 6743–6748

Torregrosa L, Bouquet A (1997) Agrobacterium rhizogenes and A. tumefaciens co-transformation to obtain grapevine hairy roots producing the coat protein of grapevine chrome mosaic nepovirus. Plant Cell Tissue Organ Cult **49:** 53–62

Torregrosa L, Iocco P, Thomas MR (2002) Influence of Agrobacterium strain, culture medium, and cultivar on the transformation efficiency of *Vitis vinifera* L. Am J Enol Vitic **53:** 183–190

Velasco R, Zharkikh A, Troggio M, Cartwright DA, Cestaro A, Pruss D, Pindo M, Fitzgerald LM, Vezzulli S, Reid J, et al (2007) A high quality draft consensus sequence of the genome of a heterozygous grapevine variety. PLoS One **2:** e1326

Verrier PJ, Bird D, Burla B, Dassa E, Forestier C, Geisler M, Klein M, Kolukisaoglu U, Lee Y, Martinoia E, et al (2008) Plant ABC proteins: a unified nomenclature and updated inventory. Trends Plant Sci **13:** 151–159

Verweij W, Spelt C, Di Sansebastiano GP, Vermeer J, Reale L, Ferranti F, Koes R, Quattrocchio F (2008) An H^+ P-ATPase on the tonoplast determines vacuolar pH and flower colour. Nat Cell Biol **10:** 1456–1462

Winefield C (2002) The final steps in anthocyanin formation: a story of modification and sequestration. Adv Bot Res **37:** 55–74

Winkel-Shirley B (2001) Flavonoid biosynthesis: a colorful model for genetics, biochemistry, cell biology, and biotechnology. Plant Physiol **126:** 485–493

Yazaki K (2005) Transporters of secondary metabolites. Curr Opin Plant Biol **8:** 301–307

Yonekura-Sakakibara K, Tanaka Y, Fukuchi-Mizutani M, Fujiwara H, Fukui Y, Ashikari T, Murakami Y, Yamaguchi M, Kusumi T (2000) Molecular and biochemical characterization of a novel hydroxycinnamoyl-CoA:anthocyanin 3-O-glucoside-6′′-O-acyltransferase from *Perilla frutescens*. Plant Cell Physiol **41:** 495–502

Zhang H, Wang L, Deroles S, Bennett R, Davies K (2006) New insight into the structures and formation of anthocyanic vacuolar inclusions in flower petals. BMC Plant Biol **6:** 29